

Evidence for cholera aggregation on GM1-decorated lipid bilayers

Rong Wang^{a,*}, Jeane Shi^b, Atul N. Parikh^c, Andrew P. Shreve^b,
Liaohai Chen^d, Basil I. Swanson^b

^a Department of Biological, Chemical and Physical Sciences, Illinois Institute of Technology,
Chicago, IL 60616, USA

^b Bioscience Division, Los Alamos National Laboratory, Los Alamos, NM 87545, USA

^c Department of Applied Science, 3001 Engineering III, University of California at Davis, Davis, CA 95616, USA

^d Biosciences Division, Argonne National Laboratory, 9700 S. Cass Avenue, Argonne, IL 60439, USA

Abstract

The binding properties of cholera toxin B (CTB) oligomer to substrate supported membrane bilayer, containing physiologically relevant concentrations of receptor glycolipids, *viz.* monosialoganglioside (GM1), have been extensively studied by the atomic force microscopy (AFM). Two distinct classes of GM1 containing membrane-mimetic surfaces were prepared: supported lipid bilayer membranes (sBLMs) on freshly cleaved mica and hybrid lipid bilayer membranes (hBLMs) on octadecyltrichlorosilane (OTS) derivatized silicon substrates. On sBLMs, aggregates with a well-defined ordered arrangement of individual CTB molecules were observed at all GM1 and cholera concentrations studied. In sharp contrast, features consistent with randomly distributed adsorbed individual CTB molecules were seen on a bare mica surface. On the hBLMs, the aggregate structures were only observed when the bilayer was formed onto ordered OTS surfaces, offering continuous and defect-free lipid membrane for the lateral diffusion of GM1. Ill-packed and disordered OTS monolayers yielded a random distribution of adsorbed proteins comparable to that observed for CTB binding on bare mica substrates. These observations strongly support that the aggregation of CTB–GM1 complex is a result of the specific interaction of CTB molecules with GM1 receptors in the fluid membrane bilayers. The high mobility of GM1 allows lateral diffusion of the complex to form ordered aggregates.

© 2003 Elsevier B.V. All rights reserved.

Keywords: Protein aggregation; Cholera toxin B oligomer; Atomic force microscopy

1. Introduction

The aggregation properties of membrane-associated proteins and peptides are often critically responsible for their biological functions. For example, both inter-leaflet dimerization and the aggregation state of gramicidin in a lipid bilayer environment may be important for the ion channel function of the peptide [1]; ordered protein aggregation was found to be a consequence of Alzheimer's disease [2]; aggregation of cell surface receptors plays essential role in initiating signal transduction [3]; pore-forming aggregation of bacterial cytotoxins (e.g., staphylococcal α -toxin, streptolysin-O, *Escherichia coli* hemolysin) generates their toxicities [4].

Many bacterial toxins are peripheral membrane proteins, and their interactions with the membrane surface are typically mediated by specific binding with membrane-incorporated receptors [5,6]. Much of the research in this context has focused on the prototypical case of cholera–GM1 interactions.

Cholera toxin is a member of the AB₅ family of bacterial toxins containing a catalytic A subunit and a homopentameric B oligomer encapsulating a central pore formed by the long α -helices on each monomer [7–9]. It is now well recognized that the cholera toxin B oligomer (CTB) participates in specific binding with ganglioside GM1 molecules present in the outer leaflets of a wide range of cell membrane bilayers. GM1 molecules contain two long hydrophobic acyl chains and a hydrophilic pentasaccharide head group. The latter is responsible for the recognition of CTB. Although the present research addresses only the interaction of the B₅ subunit with membranes, in the case

* Corresponding author. Tel.: +1-312-567-3121;

fax: +1-312-567-3494.

E-mail address: wangr@iit.edu (R. Wang).

of the full AB₅ toxin, after the CTB oligomer binds to the receptor molecules (GM1) in the cell membrane, the catalytic (cytotoxic) A subunit is translocated into the cell via an unclear endocytosis mechanism.

While a clear understanding of surface distribution (and aggregation) of cholera bound specifically to GM1 receptors has not yet emerged, the toxicity may be triggered by an aggregated structure of cholera toxin bound to the cell membrane (possibly through mediation of the endocytosis process). This belief is based on previous observations that the toxicity of many bacterial cytotoxins is initiated by protein aggregation on membrane surfaces (see above). To investigate the possibility of formation of well-defined cholera aggregate structures after binding to GM1 contained in laterally fluid membranes and to characterize these structures is a major goal of this study.

To this end, recent advances in preparing well-defined membrane-mimetic structures at solid surfaces and in imaging individual proteins at sub-molecular resolution under physiologically relevant conditions are important. For example, the techniques of Langmuir–Blodgett deposition and vesicle fusion have proved remarkably successful in preparing supported lipid bilayer membranes (sBLMs) and hybrid lipid bilayer membranes (hBLMs). Hydrophilic substrates [10,11] allow sBLMs whereas hydrophobized substrates allow hBLMs [12–14]. In the area of imaging, observation of protein assemblies with sub-molecular level resolution has been achieved by atomic force microscopy (AFM) [15]. In addition, AFM studies on the nature of ligand–receptor interaction and ligand-induced receptor behaviors are also beginning to be appreciated [16–18].

Here, we describe a study aimed directly at characterizing the lateral distribution of the CTB oligomers bound to substrate-supported lipid bilayers decorated with GM1 receptors in a physiologically relevant range (below 1 mol%) of receptor concentration. The study applies high resolution AFM measurements in aqueous ambient conditions to both sBLMs and hBLMs on planar substrates. In particular, fluid membrane mimics were derived by the fusion of 1-palmitoyl-2-oleoyl-sn-glycero-3-phosphocholine (POPC) vesicles onto hydrophilic (freshly cleaved mica) and hydrophobic (silanized silicon) substrates. The choice of POPC phospholipid was made to ensure the formation of fluid lipid layers under room temperature conditions. Tapping mode AFM measurements under buffer solution minimized tip contact with the surface structure. This is important because contact-mode AFM scans require the tip to be in contact with the surface at all times, which often perturbs surface structures by displacing weakly bound surface species, e.g. physisorbed biomolecules. On the other hand, tapping-mode AFM, where the cantilever oscillates at a high frequency so that the tip is only transiently in contact with the surface, significantly reduces tip-induced sample reconstruction. Our results reveal the emergence of well-defined aggregate clusters when continuous, fluid lipid bilayers containing low concentrations of GM1 are exposed to the CTB. As noted,

such association could play an important role in mediating the function of this membrane-associated protein.

2. Experimental section

2.1. Materials

Cholera toxin B oligomer (B₅ subunit) and ganglioside GM1 were purchased from Sigma and Matreya (Pleasant Gap, PA), respectively. 1-Palmitoyl-2-oleoyl-sn-glycero-3-phosphocholine was purchased from Avanti Polar Lipids (Alabaster, AL). Octadecyltrichlorosilane (OTS) was purchased from Aldrich. All organic solvents were HPLC grade. All chemicals were used without further purification.

2.2. Sample preparation

Supported POPC bilayers were formed using a vesicle fusion method. Briefly, small unilamellar vesicles (SUVs) were prepared by sonicating 1 mM POPC in phosphate buffered saline (PBS) solution (containing 0.0017 M KH₂PO₄, 0.005 M Na₂HPO₄, 0.15 M NaCl, pH 7.4) using a probe sonicator (Misonix, Farmingdale, NY). Pre-calculated molar percentages of (0.2–1 mol%) GM1 were added to the vesicle solutions and incubated overnight at 4 °C. Due to its amphiphilic nature, the GM1 molecules are known to spontaneously and uniformly partition into the lipid vesicles. Five microliter of this solution was then spread on a freshly cleaved mica substrate. An incubation period of 20 min was allowed to ensure that complete GM1–phospholipid bilayers were obtained on the substrate surfaces. Incomplete bilayers containing surface defects, required for control experiments, were derived by limiting the incubation period to 5 min. After bilayer deposition, the samples were then thoroughly rinsed by PBS buffer to remove any unfused vesicles from the bilayer surfaces. CTB solutions at various concentrations (as indicated in the text) were then applied to the surface. After 30 min incubation, the surface was thoroughly rinsed again by PBS buffer. With a drop of PBS buffer on the surface, the substrate was transferred to the AFM chamber for imaging.

The hybrid bilayer was similarly prepared by the surface fusion of small POPC–GM1 vesicles onto silanated silicon substrates. Silanization was achieved by assembling OTS monolayers using a Langmuir–Blodgett technique, as described in detail in our previous work [19]. Briefly, 1 mM OTS in a 2:1 (v/v) chloroform/methanol mixture was spread on the Millipore water (18 M Ω , surface tension of 72.0 mN/m) subphase surface of a Langmuir trough (NIMA Technologies, Coventry, England). With a pulling rate of 5 mm/min, a monolayer was transferred to a Si wafer at surface pressures of either 7.8 or 30 mN/m. Hybrid bilayers so obtained were incubated in CTB solution as described above. All samples were maintained hydrated under PBS buffer before AFM measurements were carried out.

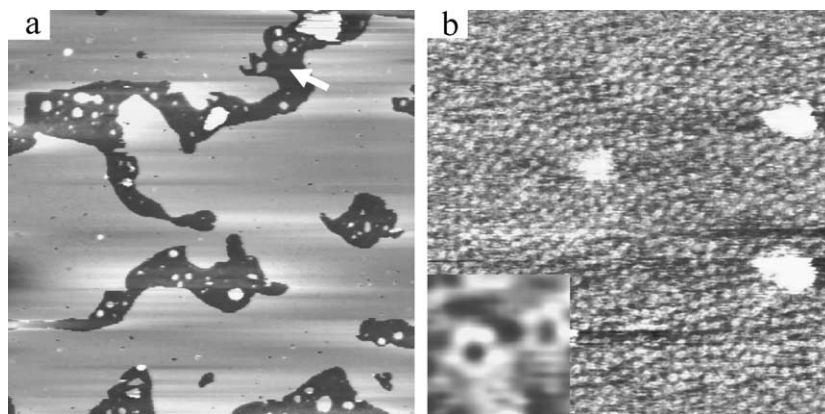


Fig. 1. (a) $3\ \mu\text{m} \times 3\ \mu\text{m}$ image of pure POPC phospholipid bilayer on mica after introducing $10^{-7}\ \text{M}$ CTB. The dark areas are bilayer defects. (b) $250\ \text{nm} \times 250\ \text{nm}$ image of a typical defect area as arrow-pointed in (a), exhibiting individual CTBs non-specifically bound to bare mica substrate. The inset of (b) shows high resolution image of a single CTB (low-pass filtered), which illustrates the central pore and the pentameric symmetry of the B oligomer. The images are in height mode.

2.3. AFM measurements

AFM measurements were carried out by using a NanoScope III system from Digital Instruments (Santa Barbara, CA). All experiments were conducted in PBS buffer solution at room temperature using a commercially available fluid cell, sealed by an O-ring. The images were acquired in the tapping-mode using the oxide sharpened Si_3N_4 tips (spring constant, $0.32\ \text{N/m}$), operating at a thermal resonance frequency of $8\text{--}10\ \text{kHz}$. Images in height mode and phase mode were collected simultaneously with 512×512 points and a scanning rate of $0.8\text{--}1.0\ \text{Hz}$ per line. All images shown are raw data except for the inset in Fig. 1b, which was low-pass filtered.

3. Results

3.1. CTB interactions with supported lipid bilayers

Fig. 1a shows a typical $3\ \mu\text{m} \times 3\ \mu\text{m}$ AFM image of a mica surface incubated first with pure POPC (without GM1) SUVs for 5 min followed by 20 min incubation with $10^{-7}\ \text{M}$ CTB solution (see sample preparation). On casual inspection, the image reveals irregularly shaped dark domains (containing occasional bright specks) within a continuous bright background. Our height measurement suggests that the bright background is topologically elevated by $5.6 \pm 0.4\ \text{nm}$ over the dark region. On the other hand, the dark (defect) domains are not featureless substrate surface. Fig. 1b shows an AFM image of the fine structure composed of a random assembly of uniform particles with the nearest neighbor distance ranging from 6.5 to 9.0 nm, and the most probable distance of $7.5 \pm 0.3\ \text{nm}$. A closer inspection of these particles (inset of Fig. 1b) clearly reveals a pentameric structure in direct correspondence with individual CTB oligomer. The topographic characteristics

of each particle, namely, $5.3 \pm 0.3\ \text{nm}$ in diameter and a central pore of $1.6 \pm 0.3\ \text{nm}$, are in direct agreement with the values for a single B_5 subunit reported previously in [17,20–23]. The height of CTB oligomer versus bare mica substrate is $1.4 \pm 0.3\ \text{nm}$. Considering the height difference of $5.6 \pm 0.4\ \text{nm}$ measured in Fig. 1a, we assign the bright background to the POPC lipid bilayer and its thickness is $7.0 \pm 0.7\ \text{nm}$. This value is approximately consistent with that reported by Jimenez-Monreal et al. [24]. They assigned the observed bilayer “thickness” to the physical height of the fluid POPC bilayer, estimated to be between ≈ 5.9 and $\approx 6.5\ \text{nm}$ [24].

It is further instructive to note that no CTB oligomers are observed over the bright background. In a control experiment, complete bilayers of pure POPC (without GM1) were formed on mica by incubating POPC vesicles for >20 min (in contrast to the 5 min process described above). Here, after incubation with CTB solution, no noticeable adsorption of CTB was observed in AFM images. Collectively, these observations indicate: (1) CTB adsorption occurs in the defect areas of POPC bilayers, presumably onto the exposed mica surface; (2) the presence of pure POPC bilayers inhibit CTB adsorption on the lipid surface; and (3) CTB adsorption on mica is characterized by the presence of unaggregated CTB molecules.

Fig. 2 displays typical AFM images obtained for mica surfaces incubated first with 1 mM POPC in buffer solution containing 1 mol% of GM1 molecules, followed by incubation with $10^{-7}\ \text{M}$ CTB solution. Fig. 2a and b shows large area images ($1.1\ \mu\text{m} \times 1.1\ \mu\text{m}$) of the same scan in the height mode and the phase mode, respectively, whereas Fig. 2c and d shows higher resolution images ($500\ \text{nm} \times 500\ \text{nm}$) of the same sample area in the height and the phase modes, respectively. The large area image in Fig. 2a clearly reveals the presence of constant-sized bright particles ($15 \pm 2\ \text{nm}$) uniformly covering the entire substrate surface. Comparing Fig. 2a with Fig. 2b, the bright particles in the height

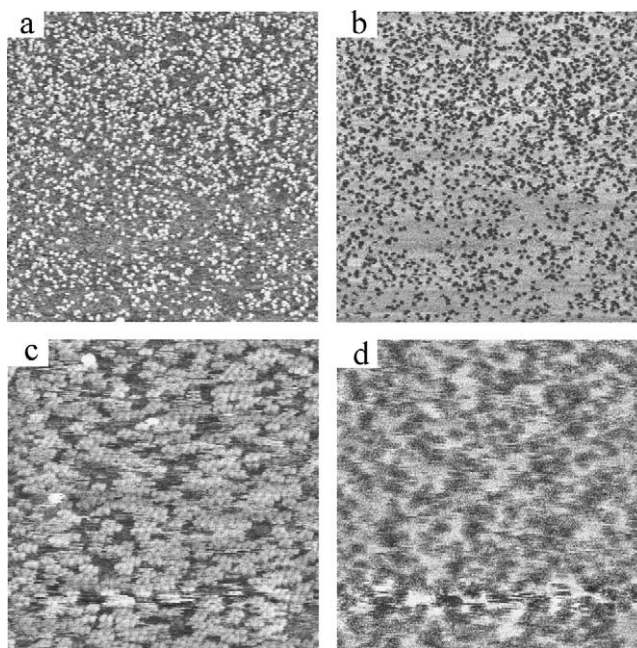


Fig. 2. CTB aggregation upon binding to GM1 that incorporated in the POPC bilayer on mica. (a) $1.1\ \mu\text{m} \times 1.1\ \mu\text{m}$ image in height mode. (b) $1.1\ \mu\text{m} \times 1.1\ \mu\text{m}$ image in phase mode. (c) $500\ \text{nm} \times 500\ \text{nm}$ image in height mode. (d) $500\ \text{nm} \times 500\ \text{nm}$ image in phase mode. CTB concentration is of $10^{-7}\ \text{M}$. GM1 (1 mol%) is involved in the POPC bilayer.

mode correspond to the dark features in the phase mode. A closer analysis of these particles using high resolution images (Fig. 2c) suggests that the particles are structured aggregates, composed of a number of closely packed smaller units. Though it is difficult to quantitatively explain phase images because different variations (e.g., softness, elasticity, hydrophilicity, chemical and topographical variations) may give rise to phase shifts of the cantilever, phase images provide a measure of sample heterogeneity [25,26]. The phase mode image in Fig. 2d shows clear contour and size of the individual aggregate embedded in POPC bilayer. Although clear sub-molecular resolution images of CTB could not be obtained under these conditions, the size of each small unit in the aggregate ($5.5 \pm 0.3\ \text{nm}$), the existence of central pore ($1.7 \pm 0.3\ \text{nm}$), and its height above the bilayer background ($1.5 \pm 0.3\ \text{nm}$) are in direct cor-

respondence with those of individual CTB proteins, seen also in Fig. 1b. The separation between the neighboring CTBs in each aggregate ranges from 5.5 to 7.5 nm, with the most probable separation of $6.0 \pm 0.3\ \text{nm}$. By comparison, a notably larger separation between unclustered CTB molecules was observed for direct adsorption on mica (Fig. 1b).

Further, AFM measurements were also conducted at lower concentrations of CTB and GM1. Fig. 3a illustrates the height image obtained when POPC bilayers containing 1 mol% GM1 was incubated with $10^{-8}\ \text{M}$ CTB solution. While the amount of CTB bound is significantly lower as the CTB concentration decreases (comparing with Fig. 2), the presence of uniformly sized aggregates is still evident. Even at the extremely low concentrations of both CTB ($10^{-9}\ \text{M}$) and GM1 (0.2 mol%), uniformly sized aggregates

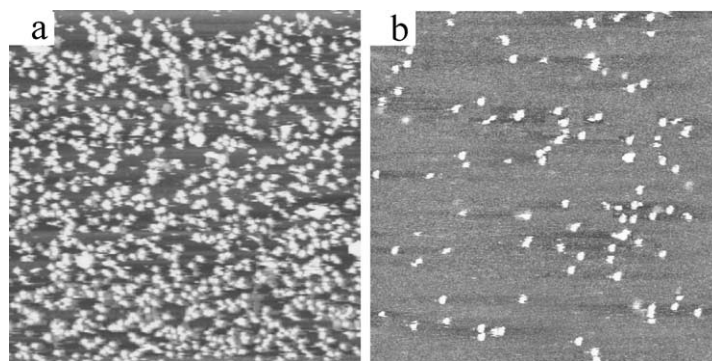


Fig. 3. CTB aggregation with (a) $10^{-8}\ \text{M}$ CTB added to POPC bilayer containing 1 mol% GM1, height image size $1.03\ \mu\text{m} \times 1.03\ \mu\text{m}$; (b) $10^{-9}\ \text{M}$ CTB added to POPC bilayer containing 0.2 mol% GM1, height image size $1.09\ \mu\text{m} \times 1.09\ \mu\text{m}$.

were observed as shown in Fig. 3b. In summary, the present series of experiments involving the characterization of CTB adsorbed on GM1-decorated, supported POPC bilayers reveal that: (1) structured aggregates of CTB are consistently observed when POPC bilayers containing low concentrations of GM1 are incubated with CTB solutions; and (2) aggregate structure is found to occur over the entire range of GM1 (0.2–1.0 mol%) and CTB (10^{-7} to 10^{-9} M) concentrations studied. These results are in contrast to those for exposed mica surface between pure POPC domains (see above) where individual molecular adsorption of CTB was observed (Fig. 1).

3.2. CTB–GM1 on OTS/POPC hybrid bilayers

As reported previously [19], an OTS monolayer prepared from a Langmuir precursor at a surface pressure of 7.8 mN/m shows concentric ring-shaped domains on a Si wafer, illustrating a nonequilibrium system with the co-existence of liquid-condensed (LC) phase, liquid-expanded (LE) phase and gas phase simultaneously. It was found recently that long-term (>8 months) storage of the samples under ambient conditions resulted in surface reorganization, presumably driven by nonequilibrium to equilibrium transformation. Fig. 4a shows the image of the resulting OTS partial monolayer, demonstrating single rings ranging from 200 to 850 nm in diameter. Height analysis indicates the areas encircled by the rings and that outside the rings have identical height, however the rings are 1.1 ± 0.2 nm higher. This suggests that the equilibrium system contains two phases: the LC phase (on the rings) and the LE phase (inside and outside the rings) [19].

Using the OTS modified Si wafer as a substrate, the vesicle fusion (POPC incorporated with 1 mol% GM1) gives rise to a planar POPC layer on top of the OTS monolayer due to the hydrophobic–hydrophobic interaction [14]. The height difference of the ring and the interior areas increases to 1.7 ± 0.2 nm, however the morphology of the ring structures does not change (image not shown here). After adding 10^{-7} M CTB solution onto the OTS/POPC hybrid bilayer,

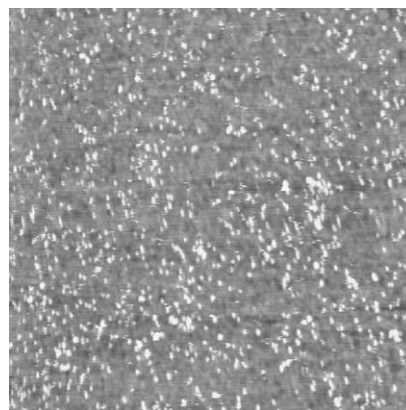


Fig. 5. $3 \mu\text{m} \times 3 \mu\text{m}$ height image of CTB aggregates on an OTS/POPC hybrid bilayer, based on a pure LC phase OTS monolayer. The POPC layer contains 1 mol% GM1. CTB concentration is 10^{-7} M.

AFM images were acquired both on top of the rings (Fig. 4b) and inside the rings (Fig. 4c) to examine the influence of the substrate property. On top of the rings, the CTBs form similar aggregates with identical height and similar size to those shown in Fig. 2. Individual B oligomer can be resolved in each aggregate. In contrast, most CTBs randomly bind to the area inside the rings as monomers (bright spots in Fig. 4c), though very occasionally CTB aggregates can also be observed in this region. The background of Fig. 4c is rougher than that of Fig. 4b because of the relative disorder of the OTS monolayer in the LE phase.

As a control experiment, a pure LC phase OTS monolayer prepared from a Langmuir precursor at a surface pressure of 30 mN/m was used as a substrate for POPC vesicle fusion. This hydrophobic surface is flat and uniform with very few defective areas. An AFM image was collected after introducing 10^{-8} M CTB to the phospholipid layer (1 mol% GM1 incorporated) and is shown in Fig. 5. CTB aggregates are evident on the surface, analogous to the features in Figs. 2, 3 and 4b.

The result of the above experiments is twofold: (1) Comparing with the LE phase OTS layer, the LC phase OTS layer offers a smooth, ordered and defect-free substrate

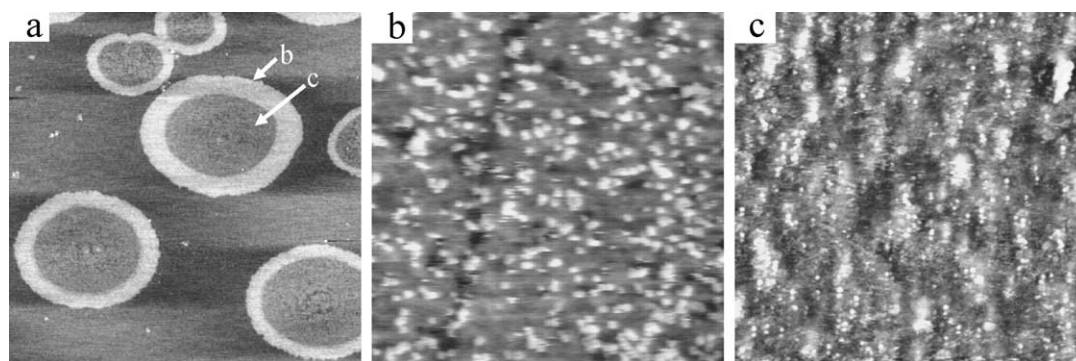


Fig. 4. (a) An OTS monolayer on silicon wafer at equilibrium state, prepared from Langmuir precursor at surface pressure of 7.8 mN/m and pulling rate of 5 mm/min; (b) and (c) CTB association with 1 mol% GM1-incorporated OTS/POPC hybrid bilayer on top of the ring and inside the ring, respectively, as arrow-indicated in (a). All the images are in height mode. The image size of (a) is $12 \mu\text{m} \times 12 \mu\text{m}$. The image size of (b) and (c) is $600 \text{ nm} \times 600 \text{ nm}$.

for vesicle fusion; (2) as a CTB solution is applied to the GM1-containing POPC/OTS hybrid bilayers, structured aggregates of CTB are consistently observed on the LC phase regions, whereas randomly distributed individual CTBs are predominant on the LE phase regions.

4. Discussion

4.1. CTB aggregation induced by specific binding

Although the interaction between individual cholera toxin proteins and GM1 has been intensively studied in many aspects [20,27,28], study of cholera–cholera association upon binding to the receptor GM1 has been neglected even though it may be of importance in initiation of toxin function. Taking advantage of the power of AFM to study biological specimens with high spatial resolution under physiological conditions, we directly observed characteristic aggregation feature of CTBs following binding to GM1 molecules on biomimic membranes (Figs. 2–5).

Fig. 2c highlights the detailed structure of the aggregates, indicating local crystallization of the CTBs. A large area of two-dimensional structured aggregate of CTB was achieved by Mou et al. [22] by involving sufficient GM1 (10 mol%) in a phospholipid bilayer. Considering that each CTB may bind up to five GM1 molecules, the size of the CTB is $\approx 25 \text{ nm}^2$ and the molecular area of the GM1 ($\approx 1 \text{ nm}^2$) is about twice of the size of the phospholipid ($\approx 0.5 \text{ nm}^2$) [29], it is estimated that 10 mol% GM1 in POPC may result in a full coverage of CTB on the bilayer. It is therefore reasonable that an ordered crystalline structure of the CTBs is established under these conditions. In our experiments, the low GM1 concentrations used allow the observation of small aggregates with local crystallization. The crystallinity of the aggregates suggests that they could act as nucleation centers for the growth of a two-dimensional array when the concentration of GM1 increases. Interestingly, when CTBs non-specifically bind to a bare mica surface, presumably via an electrostatic interaction between the negatively charged mica and the positively charged CTBs (Fig. 1b), no crystallization or aggregation is observed even though the CTBs adsorb to the surface with a very high density. On the other hand, Fig. 3 illustrates the images at lower concentrations of both CTB and GM1. The amount of surface-bound CTBs is significantly reduced (Fig. 3a and b versus Fig. 2a), however aggregation obviously happens. These imply that the CTBs do not aggregate in the solution phase before they interact with the GM1 molecules on the membrane, and the aggregation observed in Fig. 2 is not solely governed by the CTB–CTB interactions in solution. Though a recent report by Yuan and Johnston demonstrated GM1 aggregation on GM1/DPPC and GM1/egg-PC (ratios of 5:100 and 10:100, respectively) lipid bilayers prior to the CTB–GM1 binding [30], our AFM images of GM1/POPC (ratios of 1:100 to 0.2:100) bilayers showed homogeneous and uniform sur-

faces suggesting the lack of GM1 aggregation. This was confirmed by an earlier work [31] via the resonance energy transfer study. The homogeneous distribution of the GM1 molecules implies that the CTB aggregation we observed is also not caused by a pre-aggregation of GM1 on the membrane.

A plausible explanation of the CTB aggregation is that, when a CTB binds to a GM1 on lipid bilayer, the rest of the CTB binding sites have the tandem effect of attracting more GM1 molecules to the neighborhood due to the long-range specific interaction [32,33], reinforcing the local concentration of GM1 molecules. Consequently, as the GM1 molecules bind to more CTBs, more CTB–GM1 complexes form and accumulate at the local region. The enhanced surface concentration may also contribute to the aggregation of the CTB–GM1 complexes. Even in a living cell, as the proteins interact with cell membrane species via specific binding, the protein concentration will be significantly elevated on the cell surface. The relatively high surface concentration may reinforce the interaction between the neighboring CTBs, giving rise to aggregation. Without the receptors on the membrane, there is no protein adsorption (non-specific binding) for both our biomimic membrane and native cell membrane, hence no aggregation may occur. These yield the conclusion that the CTB aggregation is characteristic of CTB–GM1 specific binding. We also observed the size of the aggregates is uniform across the bilayer surface, most likely regulated by the specific interactions in the CTB–GM1 binding system. Note that the specific binding may induce conformational change of the CTB–GM1 complex, which might also favor the aggregation. However, there is currently no direct evidence to address these possibilities.

Since, neither CTB nor GM1 aggregates before specific binding happens on the POPC bilayer surface, only when the GM1 molecules can carry the bound CTBs to freely diffuse on the bilayer surface, CTB aggregates may form. The choice of using POPC to form the phospholipid bilayers assures the high surface fluidity at room temperature, which allows the GM1 molecules to keep high mobility on the surface. The lack of aggregation of CTB on bare mica surface provides support of this hypothesis. Meanwhile, the GM1 aggregation upon the CTB–GM1 specific binding under similar experimental conditions has been verified by the resonance energy transfer among the fluorescein-labeled GM1 molecules [31].

4.2. Influence of the surface fluidity on CTB aggregation

Surface fluidity of the phospholipid bilayer is important for the formation of CTB aggregates. The OTS monolayer seen in Fig. 4a contains two phases: LC phase on the rings and LE phase inside the rings. The biggest difference between the LE phase and the LC phase layer is that the OTS molecules are more densely packed and better ordered in the LC phase than in the LE phase [34,35]. The increased height difference of the two areas after POPC vesicle fusion

(from 1.1 ± 0.2 to 1.7 ± 0.2 nm) indicates that the POPC layer is better organized on the LC phase than on the LE phase. As shown in Fig. 4b, CTB–GM1 binding on the LC phase OTS/POPC results in the CTB aggregation, analogous to the features on the supported phospholipid bilayers on mica (Figs. 2 and 3). On the other hand, while CTB aggregates are occasionally observed on the LE phase OTS/POPC surface, individual CTBs with random distribution are predominant in this area (Fig. 4c). The image in Fig. 5 further identifies the aggregation characteristics when a pure LC phase OTS monolayer is employed as a substrate for assembling the POPC monolayer. The results suggest that the outer phospholipid leaflet of the well-organized OTS/POPC hybrid bilayer is comparable in surface fluidity to the supported POPC bilayer on a mica surface, so that easy diffusion of the GM1 in it can lead to CTB aggregation. Recent fluorescent recovery after photobleaching measurements of well-formed hybrid bilayers on oxide surfaces is consistent with this result [36]. In contrast, the surface of the LE phase OTS monolayer is relatively disordered. Thus, surface defects may exist and cause discontinuity and loss of fluidity within the POPC layer. Even when specific binding occurs, most CTB–GM1 complexes are spatially localized since the GM1 cannot easily diffuse laterally.

5. Conclusions

Using atomic force microscopy, we have observed CTB aggregation associated with binding of the CTBs to their receptor ganglioside GM1 molecules on the surface of laterally fluid POPC biomimetic membranes. The high mobility of GM1 molecules within the membrane allows the CTB–GM1 complexes to diffuse and aggregate. Though cholera toxin B oligomer was used for this study, aggregation upon binding to GM1 may play an important role for function of the full toxin. Future work will explore how the aggregation of cholera toxin following binding to GM1 may affect its biological functions. A number of toxins, such as heat-labile enterotoxin from *E. coli* and pertussis toxin, have structures and functions similar to cholera toxin, thus the aggregation phenomena characterized here may be of widespread relevance for understanding the functions of bacterial toxins.

Acknowledgements

This work was supported by the LDRD program at Los Alamos National Laboratory.

References

- [1] J.X. Mou, D.M. Czajkowsky, Z.F. Shao, *Biochemistry* 35 (1996) 3222.
- [2] J.D. Harper, P.T. Lansbury, *Annu. Rev. Biochem.* 66 (1997) 385.
- [3] R.G. Posner, P.B. Savage, A.S. Peters, A. Macias, J. DelGado, G. Zwartz, L.A. Sklar, W.S. Hlavacek, *Mol. Immunol.* 38 (2002) 1221.
- [4] S. Bhakdi, H. Bayley, A. Valeva, I. Walev, B. Walker, U. Weller, M. Kehoe, M. Palmer, *Arch. Microbiol.* 165 (1996) 73.
- [5] H. Lis, N. Sharon, *Chem. Rev.* 98 (1998) 637.
- [6] B.B. Finlay, S. Falkow, *Microbiol. Mol. Biol. Rev.* 61 (1997) 136.
- [7] P. Cuatrecasas, *Biochemistry* 12 (1973) 3547.
- [8] J. Holmgren, N. Lycke, C. Czerkinsky, *Vaccine* 11 (1993) 1179.
- [9] W.I. Lencer, T.R. Hirst, R.K. Holmes, *Biochim. Biophys. Acta* 1450 (1999) 177.
- [10] L. Tamm, H.M. McConnell, *Biophys. J.* 47 (1985) 105.
- [11] M. Grandbois, H. Clausen-Schaumann, H. Gaub, *Biophys. J.* 74 (1998) 2398.
- [12] E. Kalb, S. Frey, L.K. Tamm, *Biochim. Biophys. Acta* 1103 (1992) 307.
- [13] I. Reviakine, A. Brisson, *Langmuir* 16 (2000) 1806.
- [14] T.M. Winger, E.L. Chaikof, *Langmuir* 14 (1998) 4148.
- [15] D. Fotiadis, S. Scheuring, S.A. Müller, A. Engel, D.J. Müller, *Micron* 33 (2002) 385, and references therein.
- [16] Z. Shao, J. Mou, D.M. Czajkowsky, J. Yang, J.Y. Yuan, *Adv. Phys.* 45 (1996) 1, and references therein.
- [17] R. Wang, S. Vengasandra, F. Yan, *Chem. Lett.* 11 (2001) 1170.
- [18] P.E. Milhiet, V. Vie, M.-C. Giocondi, C. Le Grimmellec, *Single Mol.* 2 (2001) 109.
- [19] R. Wang, A.N. Parikh, J.D. Beers, A.P. Shreve, B. Swanson, *J. Phys. Chem. B* 103 (1999) 10149.
- [20] P.F. Luckham, K. Smith, *Faraday Discuss.* 111 (1998) 307.
- [21] J. Yang, L.K. Tamm, T.W. Tillack, Z. Shao, *J. Mol. Biol.* 229 (1993) 286.
- [22] J. Mou, J. Yang, Z. Shao, *J. Mol. Biol.* 248 (1995) 507.
- [23] R.G. Zhang, M.L. Westbrook, E.M. Westbrook, D.L. Scott, Z. Otwinowski, P.R. Maulik, R.A. Reed, G.G. Shipley, *J. Mol. Biol.* 251 (1995) 550.
- [24] A.M. Jimenez-Monreal, J. Villalain, F.J. Aranda, J.C. Gomez-Fernandez, *Biochim. Biophys. Acta* 1373 (1998) 209.
- [25] H.G. Hansma, K.J. Kim, D.E. Laney, R.A. Garcia, M. Argaman, M.J. Allen, S.M. Parsons, *J. Struct. Biol.* 119 (1997) 99.
- [26] T.A. Camesano, M.J. Natan, B.E. Logan, *Langmuir* 16 (2000) 4563.
- [27] E.A. Merritt, S. Sarfaty, F. Van Den Akker, C. L'Hoir, J.A. Martial, W.G.J. Hol, *Protein Sci.* 3 (1994) 166.
- [28] G.M. Kuziemko, M. Stroh, R.C. Stevens, *Biochemistry* 35 (1996) 6375.
- [29] P. Luckham, J. Wood, S. Froggatt, R. Swart, *J. Colloid Interface Sci.* 156 (1993) 164.
- [30] C. Yuan, L.J. Johnston, *Biophys. J.* 81 (2001) 1059.
- [31] X. Song, J. Nolan, B.I. Swanson, *J. Am. Chem. Soc.* 120 (1998) 4873.
- [32] D.E. Leckband, J.N. Israelachvili, F.-J. Schmitt, W. Knoll, *Science* 255 (1992) 1419.
- [33] R.B. Liebert, D.C. Prieve, *Biophys. J.* 69 (1995) 66.
- [34] J.Y. Fang, C.M. Knobler, *J. Phys. Chem.* 99 (1995) 10425.
- [35] K.I. Iimura, N. Suzuki, T. Kato, *Bull. Chem. Soc. Jpn.* 69 (1996) 1201.
- [36] R.A. Provencal, A.P. Shreve, unpublished data.